

# Development of a Dielectric Loaded RF Cavity for a Muon Accelerator

Katheryn Decker French

August 12, 2010

## Abstract

The building of a muon collider is motivated by the desire to collide point-like particles while reducing the limitations imposed by synchrotron radiation. The many challenges unique to muon accelerators are derived from the short lifetime of the muons. The muons must be produced, then formed into a beam and accelerated to their final energy in less than a few milliseconds in the lab frame. One idea for accomplishing this is called a helical cooling channel, and requires placing the accelerating structure in a solenoid. The RF (radio frequency) accelerating structure in a muon accelerator should be short in the longitudinal direction, small enough in the transverse direction to fit inside the solenoids of the helical cooling channel, and have the highest possible electric field gradient. A RF cavity that meets these requirements is crucial to the development of a muon collider. There is an additional constraint if an existing source of RF power is to be used, as the frequency of the lowest RF cavity mode should match the frequency of the power source. At Fermilab, the klystrons produce RF power at 800MHz. The resonant frequency of an RF cavity depends inversely on the radius of the cavity, as well as the dielectric constant of the material within the cavity. A standard vacuum cavity with a resonant frequency of 800 MHz is too large to fit within the solenoids. This paper studies one method of avoiding this limitation by placing a dielectric material within the cavity. The effect of this dielectric is modeled in Microwave Studio to determine the right size and shape for the dielectric given, and several prototype cavities are built and tested with a network analyzer. Our proof of concept experiment shows the feasibility of further developing the design of dielectric loaded RF cavities. Further work will include tests at high power, to determine the effects of a high electric field on the dielectric.

## 1 Introduction

The idea of a muon collider is motivated by the desire to collide point-like particles at multi-TeV energies while reducing the problem of synchrotron radiation. Accelerating charges lose power through synchrotron radiation proportional to  $\frac{E^4}{\rho^2 m^4}$ , where  $E$  is the particle's energy,  $m$  is the particle's mass, and  $\rho$  is the bending radius of the bending magnets. Electrons, with their low mass, will lose much more energy to synchrotron radiation than heavier particles such as protons or muons. For this reason, large circular accelerators are typically proton-proton colliders such as the LHC at CERN, or proton-antiproton colliders such as the Tevatron at Fermilab. The problem with colliding protons, is that the collision products are from the interaction between a single quark from each proton. By colliding point-like particles, their full kinetic energy can be used completely to create new particles.

Many challenges unique to muon accelerators derive from the short lifetime of the muons. The muons must be produced, cooled, then accelerated to their final energy in less than a few milliseconds in the lab frame. The muons are produced by aiming a proton beam at a fixed target to produce pions, then allowing the pions to decay into muons. The muons produced in this way occupy a large phase space, and need to be cooled as they are accelerated. A technique called ionization cooling can be used to reduce the momentum of the muons in all three dimensions, while RF (radio frequency) is used to replenish the muon's energy and accelerate the muons in the longitudinal direction. The accelerating structure is surrounded by solenoids which serve to decrease the momentum of high energy muons more than that of low energy muons, decreasing the momentum spread. This entire structure is known as a helical cooling channel [3].

The RF accelerating structure in a muon accelerator should be short in the longitudinal direction, small enough in the transverse direction to fit inside the solenoids of the helical cooling channel, and have the highest possible electric field gradient. A RF cavity that meets these requirements is crucial to the development of a muon collider.

There is an additional constraint if an existing source of RF power is to be used, as the frequency of the lowest RF cavity mode should match the frequency of the power source. At Fermilab, the klystrons produce RF power at 800MHz. The lowest mode frequency in a basic pillbox cavity is given by the equation

$$f = \frac{2.405c}{2\pi R\sqrt{\epsilon\mu}} \quad (1)$$

where  $c$  is the speed of light,  $R$  is the radius of the cavity, and  $\epsilon$  and  $\mu$  are the relative dielectric constant and magnetic permeability of the material. Since the cavity must be small in the transverse direction, a dielectric can be put inside the cavity to lower the frequency to the desired 800 MHz. Without the dielectric material, the size of the cavity required to have a mode at 800 MHz would be too large to fit inside the solenoids.

In a cavity inside a strong solenoid field, electrons emitted from the side of the cavity will be focused to the other side, where they will cascade, causing electric breakdown. In general, it is undesirable to have dielectric material in accelerating RF cavities, as the material will be heated from the rapid polarization. However, dielectrics can be used to prevent this type of breakdown. The electric field will be the strongest near the dielectric material, so it is the most likely place for breakdown to occur. However, the electrons released from the side of the cavity will be attenuated as they travel through the material, preventing breakdown.

This paper will discuss the simulating, building, and testing of several prototype dielectric loaded cavities. Some of the relevant theory in Section 2, the simulations used are discussed in Section 3, the construction of the cavities in Section 4, and the measurements done on the cavities in Section 5. Conclusions and future work are presented in Section 6.

## 2 Theory

### 2.1 Modes of RF cavities

RF cavities are essentially circular waveguides using TM (transverse magnetic field) modes. These modes can be derived using Maxwell's equations and the boundary conditions of the cavity. For a basic pillbox cavity, this can be done analytically. For a TM mode, the electric field will be in the longitudinal direction ( $z$ ), and the magnetic field will curl around this in the transverse plane. Their solutions will be in the form of Bessel functions, and the lowest resonant frequency can be

determined by finding the first zero of the bessel function appropriate for the boundary conditions. This results in Equation 1 given above. A brief derivation of the lowest TM mode can be found in Appendix A.

For a cavity with a non-trivial shape, a simulation can be used to calculate the modes numerically, but there are a few guidelines for how the shape affects the frequency. The cavity can be modeled by an LC circuit, and the resonant frequency will be

$$\omega = 1/\sqrt{LC} \quad (2)$$

where L is the inductance and C is the capacitance. The resonant frequency will increase if either L or C is decreased. L can be decreased by decreasing the radius of the cavity. C can be decreased by decreasing the width of the side plates of the cavity.

## 2.2 Quality Factor

One measure of a system's ability to store energy is  $Q$ , the quality factor. It is defined as

$$Q = \frac{\omega W}{P_{loss}} \quad (3)$$

where  $\omega$  is the frequency,  $W$  is the energy lost per cycle, and  $P_{loss}$  is the power lost. For a dielectric loaded cavity,  $Q$  is an important measure of the feasibility of the design. Much of the power will be lost in the dielectric. The above equation can be broken up into power lost into the dielectric and the wall of the cavity using  $P_{loss} = P_{wall} + P_{diel}$  [1]. This results in the equation for  $Q$ :

$$\frac{1}{Q} = \frac{1}{Q_{wall}} + \frac{1}{Q_{diel}}. \quad (4)$$

The  $Q$  of the dielectric is given by the loss tangent, as  $Q_{diel} = 1/\tan\delta$ . The  $Q$  of the dielectric is expected to be the dominant factor in the  $Q$  of a dielectric loaded cavity, so this can be used to determine the maximum loss tangent a dielectric material can have in order to be feasible for an RF cavity in a muon accelerator.

## 2.3 S-parameters

S-parameters describe the relation between the input and output voltages of a system. For a system with two ports, the input and output voltages are related by the matrix equation:

$$\begin{pmatrix} b1 \\ b2 \end{pmatrix} = \begin{pmatrix} S11 & S12 \\ S21 & S22 \end{pmatrix} \begin{pmatrix} a1 \\ a2 \end{pmatrix} \quad (5)$$

where b1 and b2 are output voltages for ports 1 and 2, and a1 and a2 are input voltages. S11 and S22 represent the reflection coefficients for the ports, while S21 represents the forward voltage transmission, and S12 the backwards voltage transmission.

This can be generalized for an N port system, and one can write an NxN matrix. For a reciprocal system, the matrix will be symmetric, and for a lossless system, the matrix will be unitary. By measuring the change in the S-parameter matrix with frequency, the frequency response of the system can be easily understood.

Simulations for three cavity designs

Build	Width (mm)	$f_{sim}$ (MHz)	$Q_{wall}$	$Q_{total}$
1	79	789	19,170	6572
2	91	740	19,303	6587
3	86	756	17,793	6402

Table 1: Results from Microwave Studio simulation of the resonant mode frequencies and quality factors for the three cavities, assuming  $\epsilon = 9.7$  and  $\tan \delta = 0.0001$ .

Determination of  $\epsilon$  for three cavity designs

Build	$f_{obs}$ (MHz)	$\epsilon$
1	836	7.4
2	785	7.5
3	807	7.3

Table 2: Values of  $\epsilon$  required of each cavity build to reconcile the difference between the observed and simulated resonant frequencies.

### 3 Modeling and Simulations

A program called Microwave Studio, made by CST is used to simulate the electric and magnetic fields inside the cavity. The geometry of the cavity can be drawn, with materials of specified properties. Two analyses are done of the cavity. The first uses the eigenmode solver to calculate the resonant frequency of the cavity and the quality factor. The second uses the transient solver to calculate the S- parameters by modeling the power inputs through the cavity’s antennas.

The geometry of the first build of the cavity input into the model can be seen in Figure 1. The radius is 104 mm and the width is 79 mm. The dielectric has a relative dielectric constant of 9.7. This results in a predicted resonant frequency of 757 MHz. The eigenmode solver uses the AKS (Advanced Krylow Subspace) algorithm, and ignores the losses in the materials when calculating the frequency. A separate solver is used to find the Q. For this simulation, the loss tangent of the material is  $\tan(\delta) = 0.0001$ . The Q is calculated to be  $Q = 6572$  for the lowest mode. The simulated data for other builds of the cavity can be seen in Table 1.

The power input into the cavity is simulated using waveguide ports over coaxial antennas, and is shown in Figure 2. The transient solver calculates the fields and energy transmission in the time domain. The predicted S-parameters as a function of frequency over the range of 0.1 to 2 MHz can be seen in Figure 3. An electric field probe is placed in the center of the cavity to record the magnitude of the electric field in the longitudinal direction. The results from this probe in the simulation can be seen in Figure 4.

### 4 Construction of Cavity

The cavity was constructed around an existing setup of a ceramic cylinder between two copper pipes, shown in Figure 5. The ceramic was attached using a vinyl acetate seal. Alumina 99.5% was used for the ceramic. It has a relative dielectric constant of  $\epsilon = 9.7$  and a loss tangent of  $\tan \delta = 0.0001$  given by the manufacturer, measured at 1 MHz. The rest of the cavity was designed in microwave studio, and constructed out of two copper side plates and a strip of copper around the

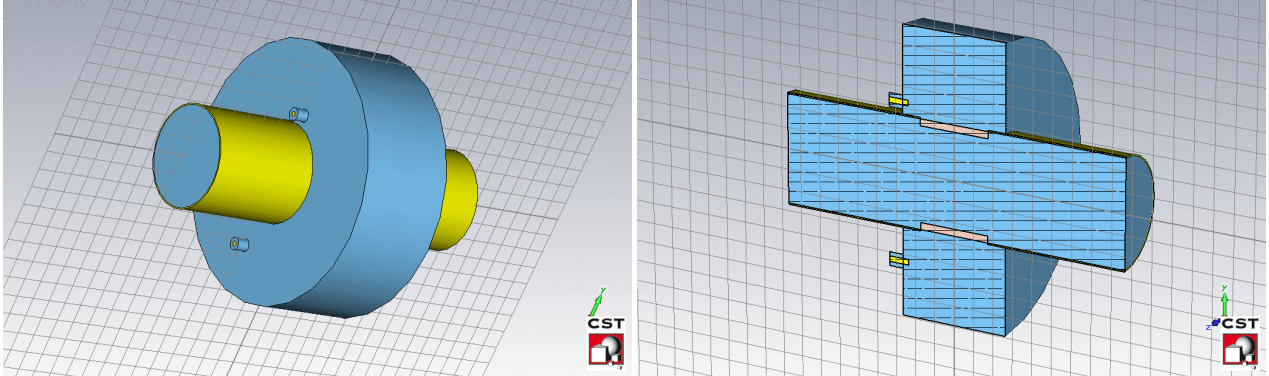


Figure 1: Geometry of first cavity in simulation. The picture on the right shows a cutout. The yellow is copper, the blue is vacuum, and the pink is ceramic. The background material is perfectly conducting.

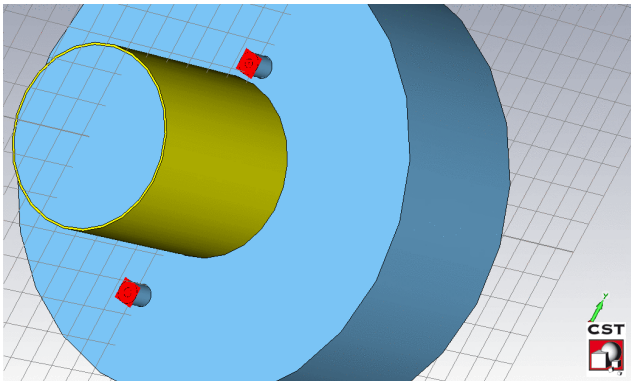


Figure 2: Waveguide ports over coaxial antennas in simulation. The ports appear as red squares.

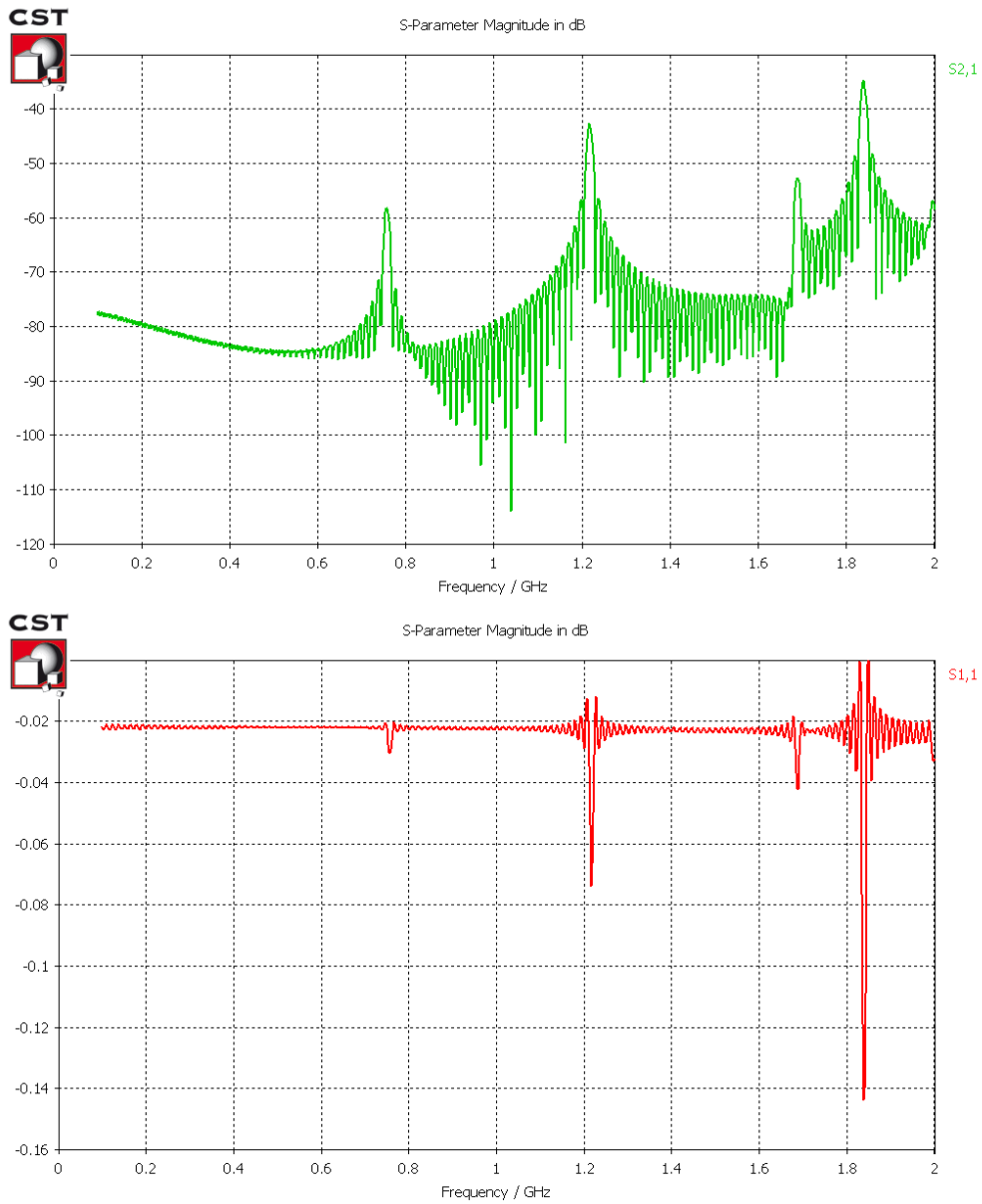


Figure 3: S- parameters for simulation of cavity build 1. S<sub>2,1</sub> is on the top, and S<sub>1,1</sub> is on the bottom.

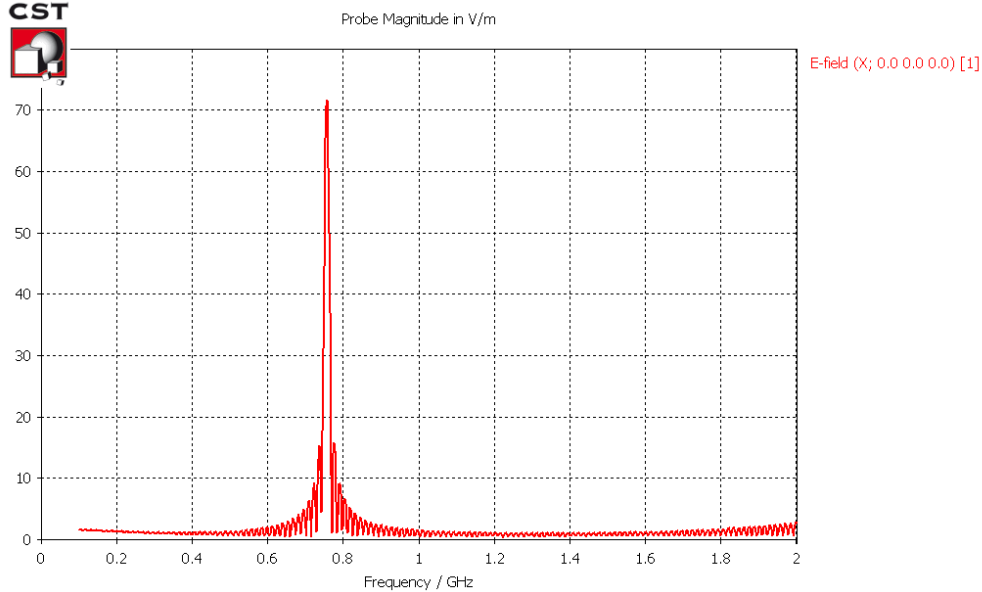


Figure 4: Results from simulated E field probe in longitudinal direction for simulation of cavity build 1.

outer edge, as shown in Figure 5. Here, the copper side plates are slightly wider than the ceramic tube. Power was fed into the cavity and measured using two antennas. The antennas and their placement are shown in Figure 6.

## 5 Experiment and Results

Properties of the cavity were measured using a network analyzer. The setup is shown in Figure 7. A full two-port calibration was used, as well as averaging in order to reduce systematic and statistical error respectively.

The resonant frequency and  $Q$  were measured for the first build of the cavity using the forward transmission parameter  $S_{21}$ . The scan over 3 kHz to 3 GHz can be seen in Figure 8, and the close up scan can be seen in Figure 9. The width is calculated by finding the points -3 dB from the maximum. The center is calculated to be  $f = 836.14$  MHz, with a bandwidth of  $bw = 1.43$  MHz, and a  $Q$  of  $Q = 583.72$ .

The discrepancy between the observed ( $f = 836$  MHz) and simulated ( $f = 789$  MHz) results prompted the building of subsequent cavities. The cavity was rebuilt twice with different widths between the side plates. The source of the frequency difference is believed to be a possible change in the dielectric constant at high frequencies. Our measurements provided three data points for determining what  $\epsilon$  would need to be in order to account for these discrepancies. Results can be seen in Table 2. The necessary value is  $\epsilon = 7.4 \pm 0.1$ .

After measuring the third build of the cavity, held together by copper tape, the cavity was soldered shut in order to determine a more realistic value of  $Q$ . The  $Q$  measured for this cavity was



Figure 5: Photo of existing copper pipe with ceramic insert (left), and photo of cavity, preliminarily held together with copper tape (right).

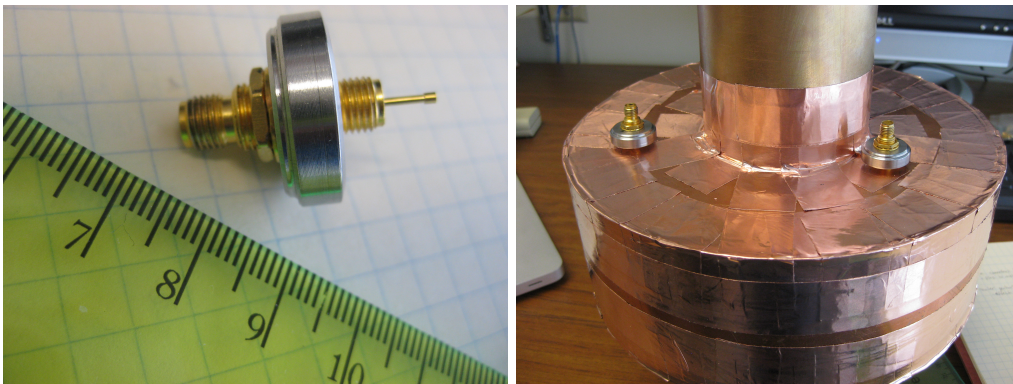


Figure 6: Photos of antenna (left), and placement of antennas in cavity (right).

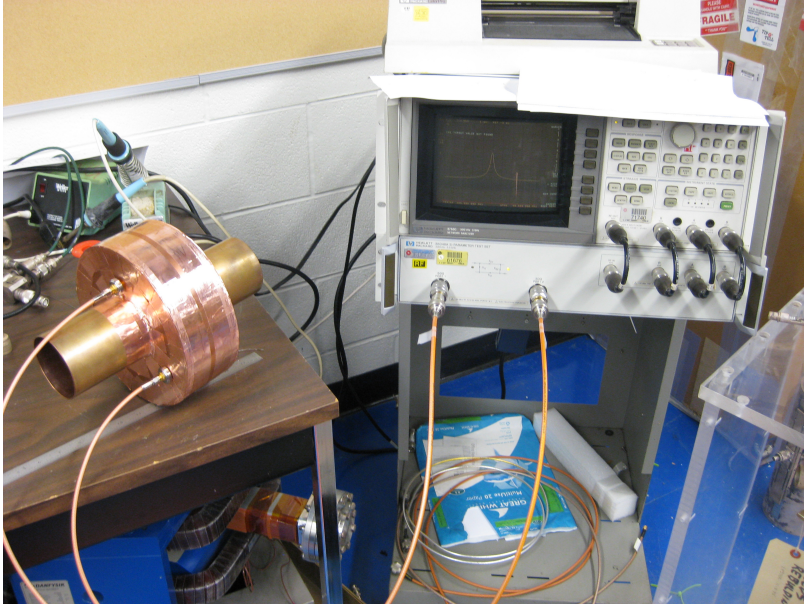


Figure 7: Photo of cavity attached to network analyzer for measurements.

$Q = 439$ . More precise machining will be required to raise the  $Q$  to a value such that it is limited only by the dielectric.

## 6 Conclusions and Future Work

This series of prototype loaded dielectric RF cavities demonstrates the feasibility of developing such cavities for a muon accelerator. One of the biggest challenges in implementing dielectric loading of cavities will be to find the right material for the dielectric. The material must have both a high dielectric constant  $\epsilon$  and a low loss tangent  $\tan \delta$  at high frequencies [1]. The relative dielectric constant was observed here to vary by more than 2 between the observed value at 800 MHz and the manufacturers value at 1 MHz.

The next step in this project after the low power network analyzer tests is to perform tests at high power at the MTA (muon test area) at Fermilab. These tests will be able to study the energy loss in the cavity from the dielectric, and further determine the feasibility of dielectric loaded cavities and the type of materials which can be used. The  $Q$  is expected to be dominated by the effect of losses in the dielectric, and will be an important measurement.

With respect to the design of the cavity, the next step is to try filling the body of the cavity with oil (or some other liquid dielectric). This would be separated from the vacuum in the beam pipe by the ceramic. The oil will serve several purposes. It can be circulated to cool the ceramic as it is heated by the RF, and it will also help prevent breakdown by attenuating electrons released from the cavity wall.

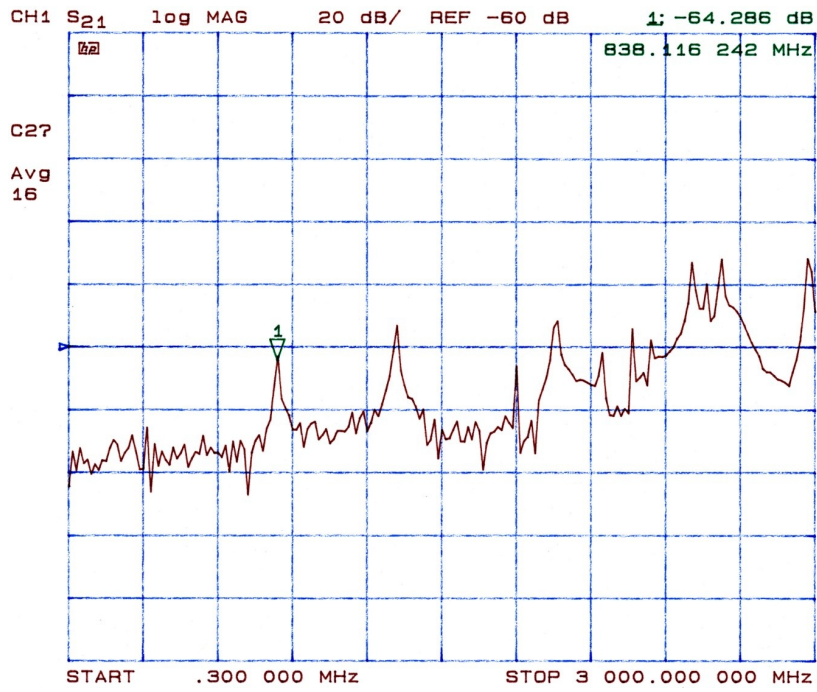


Figure 8: Network analyzer measurement of S<sub>21</sub> of the first build of the cavity. The horizontal scale is from 3 kHz to 3 GHz. The vertical scale is in units of 20 dB/division.

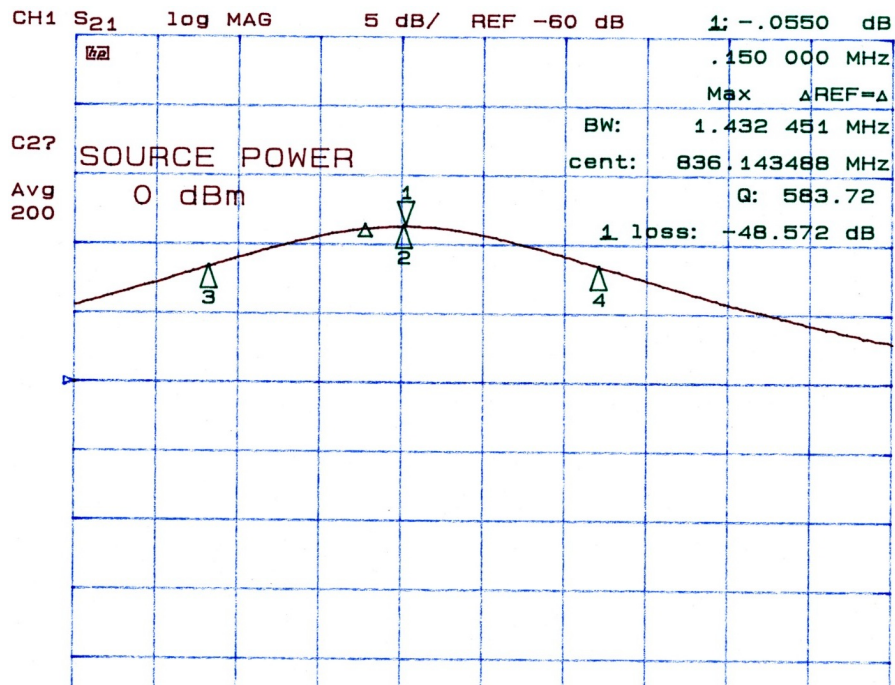


Figure 9: Network analyzer measurement of S<sub>21</sub> of the first build of the cavity. The horizontal scale is centered at 836.45 MHz with a span of 3 MHz. The vertical scale is in units of 5 dB/division.

## Acknowledgments

I would like to acknowledge Andrew Feld for his work constructing the cavity, Milorad Popovic for advising me, William Barletta for his helpful edits and project ideas, and the Lee Teng internship program for the opportunity to participate in this research.

## References

- [1] M. Popovic, A. Moretti, C. Ankenbrandt, M. Cummings, R. Johnson, and M. Neubauer. Di-electric loaded rf cavities for muon facilities. *Proceedings of IPAC10, Kyoto, Japan, 2010*.
- [2] D. Pozar. *Microwave Engineering*. Wiley, third edition, 2005.
- [3] K. Yonehara, R. P. Johnson, M. Neubauer, and Y. S. Derbenev. A helical cooling channel system for muon colliders. *Proceedings of IPAC10, Kyoto, Japan, 2010*.

## Appendix A: Derivation of lowest TM mode frequency

This is a brief derivation of the TM010 mode of a pillbox cavity, using Pozar [2] and notes from my advisor, Milorad Popovic.

TM010 is the lowest TM mode, and will have a magnetic field in the transverse directions, with  $H_z = 0$ , and an electric field in the z- direction only.

Let's do this in CGS. Assuming the absence of free charges and a  $\exp(j\omega t)$  time dependence of the fields, Maxwell's equations are:

$$\nabla \cdot B = 0, \nabla \times E = j\frac{\omega}{c}B, \nabla \cdot E = 0, \nabla \times B = -j\mu\epsilon\frac{\omega}{c}E. \quad (6)$$

The two curl equations can be broken up into their components to get six equations. Assuming a propagation in the z- direction of  $\exp(-i\beta z)$ , one can solve for the transverse field components in terms of the longitudinal field components. It will be convenient to use cylindrical coordinates due to the cylindrical symmetry of the problem.

$$E_\rho = -\frac{j}{k_c^2} \left( \beta \frac{\partial E_z}{\partial \rho} + \frac{\omega\mu}{\rho c} \frac{\partial H_z}{\partial \phi} \right), \quad (7)$$

$$E_\phi = \frac{-j}{k_c^2} \left( \frac{\beta}{\rho} \frac{\partial E_z}{\partial \phi} - \frac{\omega\mu}{c} \frac{\partial H_z}{\partial \rho} \right), \quad (8)$$

$$H_\rho = \frac{j}{k_c^2} \left( \frac{\omega\epsilon}{\rho} \frac{\partial E_z}{\partial \phi} - \frac{\beta}{c} \frac{\partial H_z}{\partial \rho} \right), \quad (9)$$

$$H_\phi = -\frac{j}{k_c^2} \left( \omega\epsilon \frac{\partial E_z}{\partial \rho} + \frac{\beta}{\rho c} \frac{\partial H_z}{\partial \phi} \right) \quad (10)$$

where  $k_c^2 = k^2 - \beta^2$ , and  $k = \omega\sqrt{\mu\epsilon}$ .

Equation 6 can also be used to derive equations for electromagnetic wave propagation:

$$\left( \nabla^2 + \mu\epsilon\frac{\omega^2}{c^2} \right) E = 0, \left( \nabla^2 + \mu\epsilon\frac{\omega^2}{c^2} \right) B = 0 \quad (11)$$

which can again be separated into equations for each orthogonal component.

Because we are considering the TM modes, we will use the equation for electric field propagation. This gives an equation for Ez,

$$\left( \frac{\partial^2}{\partial \rho^2} + \frac{1}{\rho} \frac{\partial}{\partial \rho} + \frac{1}{\rho^2} \frac{\partial^2}{\partial \phi^2} + \frac{\partial^2}{\partial z^2} + \mu \varepsilon \frac{\omega^2}{c^2} \right) \text{Ez} = 0. \quad (12)$$

We will assume that the field solutions are separable, and can be written as

$$\text{Ez} = R(\rho)Q(\phi)e^{-j\beta z + j\omega t} \quad (13)$$

and that the variation in  $\phi$  can be expressed by plane waves

$$Q(\phi) = e^{\pm im\phi}. \quad (14)$$

The differential equation now becomes

$$\left( \frac{\partial^2}{\partial \rho^2} + \frac{1}{\rho} \frac{\partial}{\partial \rho} - \frac{m^2}{\rho^2} - \beta^2 + \mu \varepsilon \frac{\omega^2}{c^2} \right) R(\rho) = 0. \quad (15)$$

Solutions to this differential equation are bessel functions.

$$R(\rho) = AJ_m(\gamma\rho) + BY_m(\gamma\rho), \quad (16)$$

$$\gamma^2 = \mu \varepsilon \frac{\omega^2}{c^2} - \beta^2 \quad (17)$$

We now have an equation for Ez,

$$\text{Ez}(\rho, \phi, z, t) = (AJ_m(\gamma\rho) + BY_m(\gamma\rho)) e^{-j\beta z + j\omega t}. \quad (18)$$

Because we are concerned with the lowest mode of the cavity,  $m = 0$ .

For a cavity made of some dielectric, surrounded by a perfectly conducting material, the Y bessel functions will be unphysical, since they go to infinity at 0,  $Y_m(0) = \infty$ . Thus the electric field will be

$$\text{E}\rho = 0, \text{E}\phi = 0, \text{Ez} = E_0 J_0(\gamma\rho) e^{-j\beta z + j\omega t}. \quad (19)$$

To find the value of  $\omega$ , we find the location of the first zero in the bessel function. This is just a constant, which depends on m. For m=1, the first zero  $J_0(x) = 0$  is at  $x=2.405$ . Because n=1, this first zero will occur at the boundary. For a cylinder of radius a,

$$J_0(\gamma a) = 0 \quad (20)$$

$$\gamma a = 2.405. \quad (21)$$

Remembering that  $\gamma^2 = \mu \varepsilon \frac{\omega^2}{c^2} - \beta^2$  and solving for the frequency  $f = \frac{\omega}{2\pi}$ ,

$$f = c \frac{\sqrt{\frac{2.405^2}{a^2} + \beta^2}}{2\pi \sqrt{\varepsilon \mu}} \quad (22)$$

For the TM010 mode,  $\beta = 0$ , so

$$f = \frac{2.405c}{2\pi a \sqrt{\varepsilon \mu}} \quad (23)$$